Catalysis Today 156 (2010) 288–294

Contents lists available at ScienceDirect

Catalysis Today

journal homepage: www.elsevier.com/locate/cattod

Catalytic properties of benzene hydroxylation by TS-1 film reactor and Pd–TS-1 composite membrane reactor

Xiaobin Wang[a], Yu Guo[a], Xiongfu Zhang[a,*], Yao Wang[a], Haiou Liu[a], Jinqu Wang[a], Jieshan Qiu[a], King Lun Yeung[b,1]

[a] State Key Laboratory of Fine Chemicals, School of Chemical Engineering, Dalian University of Technology, No. 158 Zhong Shan Road, Dalian, Liao Ning 116012, PR China
[b] Department of Chemical and Biomolecular Engineering, The Hong Kong University of Science and Technology, Clear Water Bay, Kowloon, Hong Kong, SAR, PR China

ARTICLE INFO

Article history:
Available online 14 April 2010

Keywords:
Film
Composite membrane
TS-1
Pd membrane
Catalytic membrane reactor

ABSTRACT

Titanium silicalite-1 (TS-1) and mesoporous TS-1p were incorporated as catalyst for the direct hydroxylation of benzene to phenol in a palladium membrane reactor. The zeolite also served as intermediate support layer and diffusion barrier against contaminants. Pd–TS-1 and Pd–TS-1p were characterized and tested for hydrogen permeation before investigating their performance for the benzene direct hydroxylation reaction. The effects of reactor configuration, reaction conditions and catalysts on conversion, product yield and water production were examined. The phenol yield of Pd–TS-1p was the highest followed by Pd–Sil-1 and Pd–TS-1 with Pd–TS-1p and Pd–TS-1 having phenol selectivity higher than 95%. The optimum reactor configuration and H_2/O_2 molar feed ratio were identified.

1. Introduction

Phenol is mainly produced by the energy-intensive cumene process and this motivates research into cleaner and more energy efficient processes. A single step synthesis routes based on H_2O_2 and N_2O as oxidant are attractive [1–4], but considerable economic advantages could be gained if oxygen could be used. There is growing number of reports on phenol production from H_2/O_2 mixtures over precious metal catalysts [5–7]. However, the operation is restricted by the flammability of the reaction mixture and the need for acid solvent. A new synthetic route was introduced by Niwa et al. [8] using Pd membrane to separate and control the reaction between H_2 and O_2 to generate 'in situ' H_2O_2 for the direct hydroxylation of aromatic compounds. It is a clean and economically-attractive process. Although the benzene conversion in the Pd membrane reactor can be high, the hydrogen efficiency was low and the production rate of water was 500–1000 times that of phenol [9–12]. Therefore, the phenol productivity must be improved.

Zeolites can catalyze many reactions and several works have been published reporting the performance of zeolite films and membranes for reactions and separations [13–17]. The TS-1 zeolite is an active catalyst for the selective oxidation of organics using hydrogen peroxide. The framework titanium atom is identified to be active site for the reaction. It is known to generate Ti peroxo species (Ti-OOH) with H_2O_2 before reacting with neighboring hydroxyls to form a stable complex of five-membered ring structure [18–20]. TS-1 films and membranes were grown on various supports and used to catalyze various reactions [21–25]. Yeung and co-workers [26–28] investigated epoxidation and selective oxidation reactions over TS-1 films and membranes in microreactors and our recent works reported the performance of TS-1 membranes for phenol and styrene hydroxylation reactions [29,30].

This work explores the use of titanium silicalite-1 (TS-1) zeolites as catalyst for the direct hydroxylation of benzene to phenol using oxygen and hydrogen as co-reactants. The zeolite also serves as intermediate support layer and diffusion barrier for the palladium membrane in the Pd–TS-1 composite membrane. Since TS-1 zeolite stabilizes reactive oxygen species, it is expected that it would improve the reaction for the direct hydroxylation of aromatics. The effect of reactor configuration, reaction conditions and catalysts on conversion, product yield and water production are examined. A mechanism is proposed to explain the observed reaction behavior.

2. Experimental

2.1. Materials

The α-Al_2O_3 tubes from Fo Shan (Guangdong, China) with inner and outer diameters of 9 and 13 mm respectively and a length of 75 mm were used for membrane support. The tubes have pores of 3–5 μm and a porosity of 40%. The chemicals for mem-

* Corresponding author. Tel.: +86 411 39893605; fax: +86 411 39893605.
E-mail addresses: xfzhang@dlut.edu.cn (X. Zhang), kekyeung@ust.hk (K.L. Yeung).
[1] Tel.: +852 2358 7123; fax: +852 2358 0054.

0920-5861/$ – see front matter © 2010 Elsevier B.V. All rights reserved.
doi:10.1016/j.cattod.2010.03.034

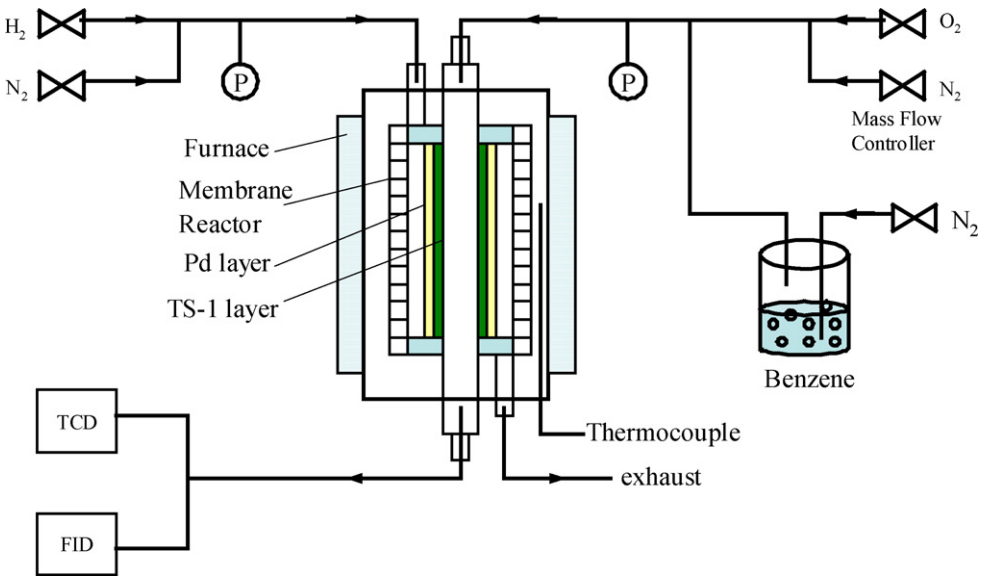

Fig. 1. Schematic of experiment apparatus used in this work.

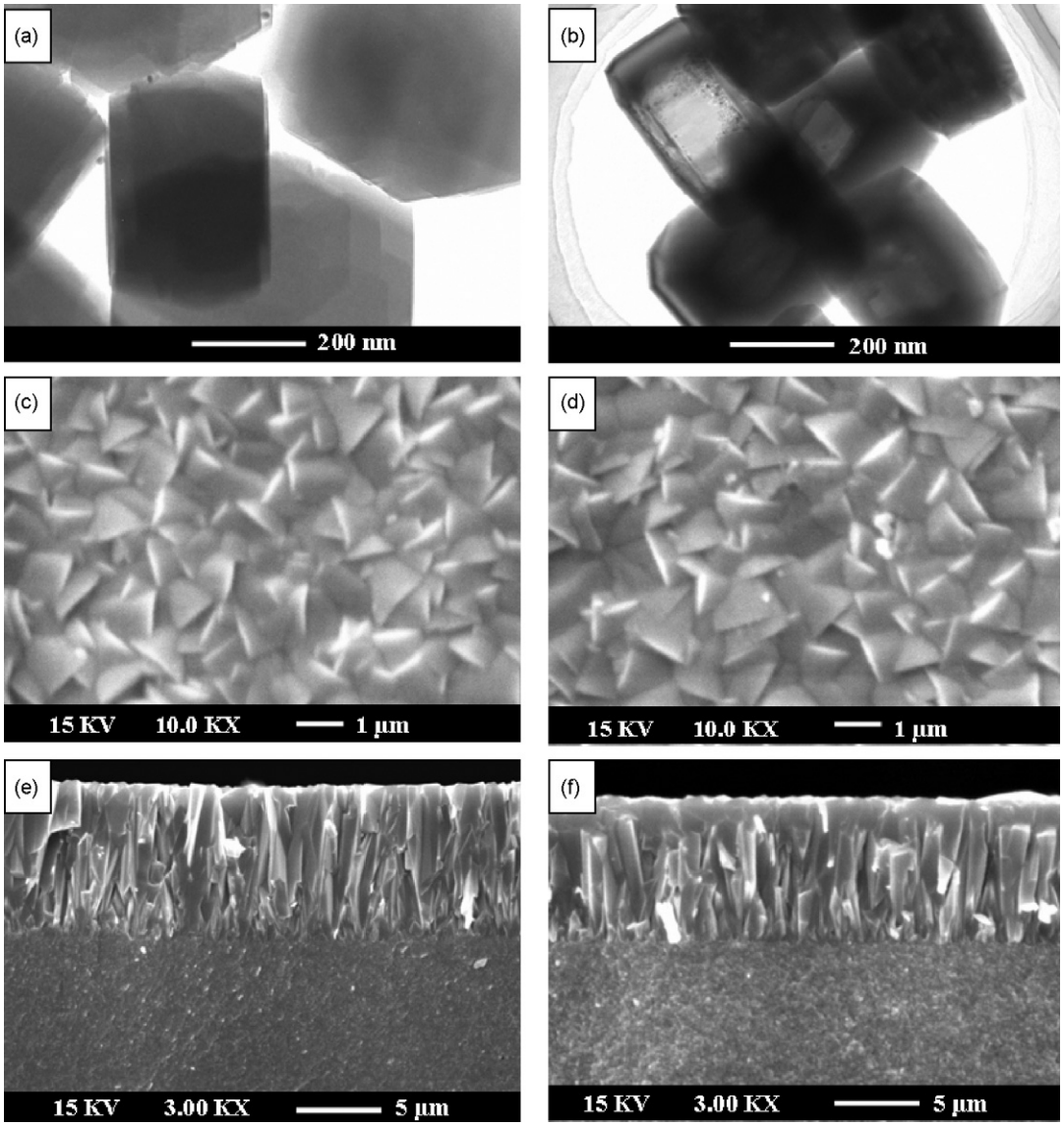

Fig. 2. TEM micrographs of TS-1 zeolite before (a) and after (b) post-treatment; SEM images of TS-1 films before ((c) surface and (e) cross-section) and after ((d) surface and (f) cross-section) post-treatment.

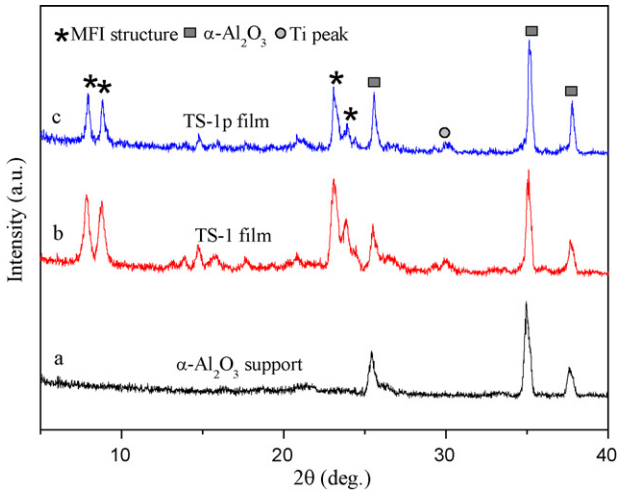

Fig. 3. XRD patterns of the support (a) and TS-1 film before (b) and after (c) TPAOH treatment.

brane preparation were purchased from Tianjian Kermel Chemical Reagent Ltd. Co. and included tetraethyl orthosilicate (TEOS), tetrabutyl orthotitanate (TBOT), palladium chloride ($PdCl_2$), tin chloride dehydrate ($SnCl_2{\cdot}2H_2O$), $Na_2EDTA{\cdot}2H_2O$ ($C_{10}H_{14}N_2Na_2O_8{\cdot}2H_2O$), hydrazine ($N_2H_4$), benzene ($C_6H_6$). The 17 wt.% tetrapropylammonium hydroxide (TPAOH) was prepared in the laboratory.

2.2. Preparation of TS-1 and Pd–TS-1 composite membranes

The detailed procedure for support pretreatment, seeding and growth of TS-1 films were described in a prior work [29]. The tubes were end-sealed leaving a 30 mm porous section and a membrane area of 12.2 cm^2. The support was seeded to eliminate unwanted contribution from the support [31] and to control the growth of the zeolite [32–36]. The TS-1 was grown from a synthesis solution of 1 SiO_2:0.02–0.03 TiO_2:0.18 TPA_2O:250 H_2O under hydrothermal conditions. Post-treatment of TS-1 film (TS-1p) in 0.5 M TPAOH solution introduced mesopores and increased site accessibility. The treatment was carried out in an autoclave containing 60 ml TPAOH solution (17 wt.%) and 42 ml distilled water at 448 K for 24 h. The prepared sample was then washed with distilled water, dried in an oven at 383 K and calcined in air at 823 K for 6 h.

The palladium membrane was deposited on the TS-1 film by electroless plating method [37–41]. The TS-1 was first seeded by a sequential immersion in $SnCl_2$ and $PdCl_2$ solutions for 10 times. Each dipping lasted for 4 min and was followed by a rinsing step in distilled water. The palladium was deposited from an electroless plating solution containing $PdCl_2$, EDTA·2Na, $NH_3{\cdot}H_2O$ and N_2H_4 at 318 K. The membrane was rinsed with deionized water and dried in the oven at 393 K. The Pd membranes deposited on the TS-1 and TS-1p zeolite layer were respectively designated as Pd–TS-1 and Pd–TS-1p composite membranes. Comparisons were made with Pd–Sil-1 membrane prepared by depositing 5 μm Pd on 2 μm Sil-1. The membranes were examined by KYKY-2008B scanning electron microscopy (SEM) and characterized by D/Max 2400 Rigaku X-ray diffractometer with a Cu-Kα X-ray radiation (XRD, λ = 0.1542 nm). The TS-1 and TS-1p were analyzed by Bruker EQUINOX55 Fourier transformed infrared spectrometer and JASCO V-550 UV-Vis spectrometer. Nitrogen physisorption (Autosorb-1) were performed on the powder samples from the membrane.

2.3. Hydroxylation of benzene to phenol

The direct hydroxylation of benzene to phenol was performed with hydrogen and oxygen gases as co-reactants in the membrane reactor shown in Fig. 1. The hydrogen permeation at different transmembrane pressures and temperatures was measured prior to the reaction. The reaction was conducted at 473 K and the H_2 and O_2

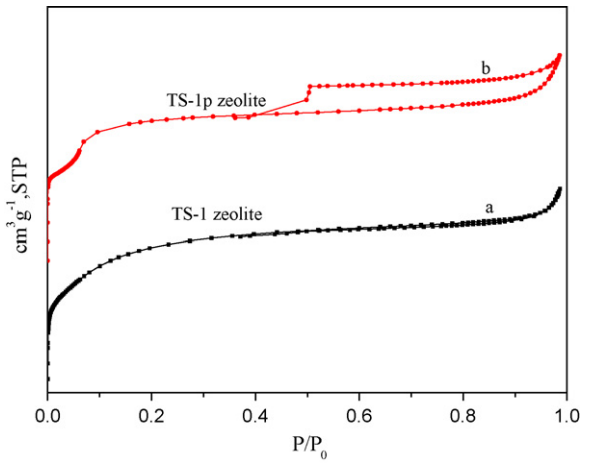

Fig. 4. Nitrogen adsorption/desorption isotherms of TS-1 zeolite before (a) and after (b) post-treatment.

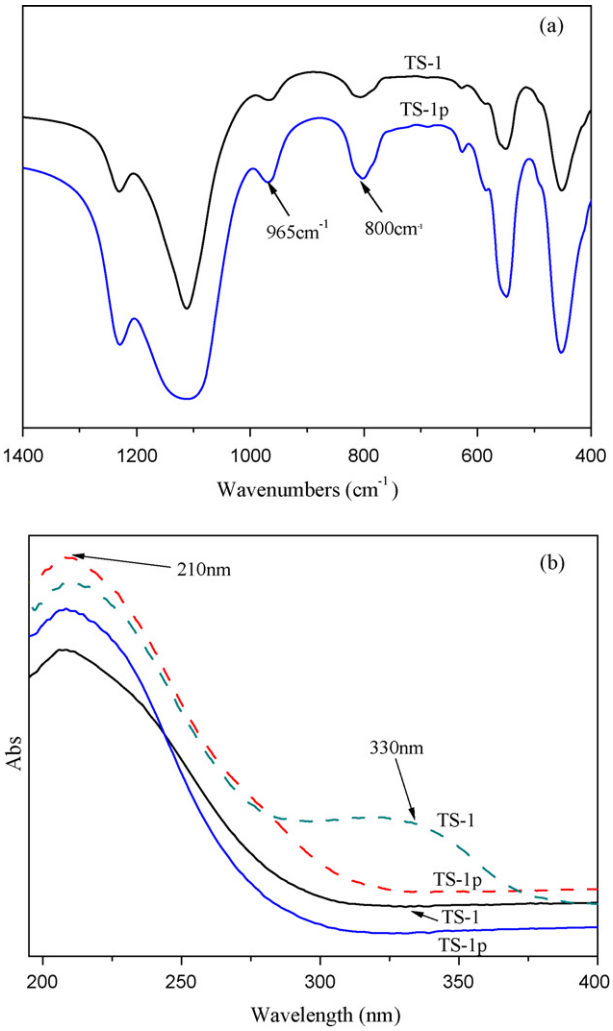

Fig. 5. The FT-IR (a), UV–Vis (b) spectra of the TS-1 zeolite (Ti/Si = 0.02: full line and Ti/Si = 0.03: dotted line) before and after TPAOH treatment.

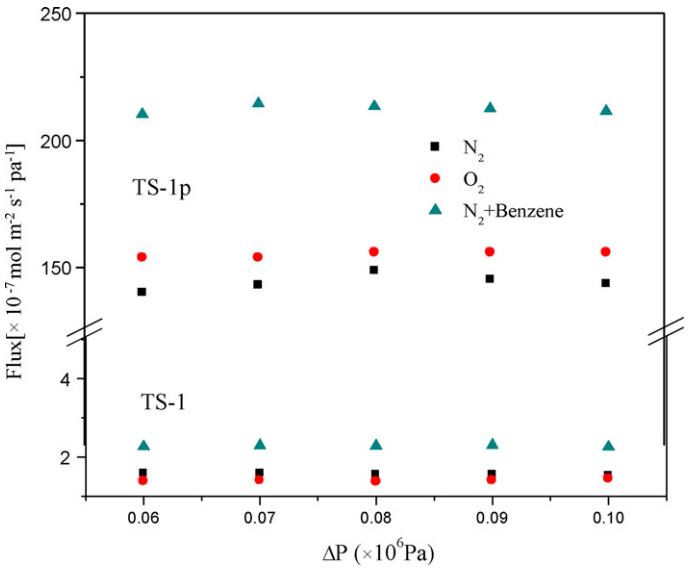

Fig. 6. The flux of reactants through TS-1 film layer before and after TPAOH treatment.

reactants were metered by mass flow controllers. The benzene was fed to reactor by bubbling nitrogen carrier gas through benzene saturator. The reaction was monitored by two online gas chromatographs (GC-7890T; GC-7890F). The inorganic products were analyzed by thermal conductivity detector (TCD) with a 13X molecular sieve and a GDX molecular sieve packed columns, while the organic products were separated by 50 m SE-30 capillary column and analyzed by the FID.

3. Results and discussion

3.1. Supported TS-1 film

Fig. 2 compares the TS-1 before and after treatment in TPAOH. Ogura et al. [42] reported that ZSM-5 treated with sodium hydroxide exhibited increased inter-grain porosity and numerous surface cracks and defects. The transmission electron microscope images in Fig. 2a and b show the TS-1 crystals before and after TPAOH treatment respectively. The formation of internal pores and voids are evident in the TS-1p zeolites as shown in Fig. 2b, but the original size and shape of the crystals (cf. Fig. 2a) remained unchanged. It is believed that the intra-particle voids are formed by a dissolution–recrystallization process [43], where the nonuniform framework composition leads to a preferential etching as shown in Fig. 2b. The effects of TPAOH treatment of TS-1 films are not apparent from the SEM images of the film surface (Fig. 2c and d) and cross-sections (Fig. 2e and f). The film morphology, grain intergrowth and crystal orientation are identical for the TS-1 and TS-1p films.

The X-ray diffraction data in Fig. 3 show that TS-1p has weaker diffraction signal with a significant decrease in peak intensity of (0 3 3) that could be evident of selective etching. The X-ray diffraction peak at $2\theta = 29.3^\circ$ is generally attributed to titanium incorporated in MFI framework and is present in both TS-1 and TS-1p. The nitrogen physisorption isotherms of TS-1 and TS-1p powders are plotted in Fig. 4. TS-1 displays a Type-I isotherm (Fig. 4a) that is typical of zeolites, while TS-1p exhibits a H2 hysteresis loop from mesopores created after the TPAOH treatment (Fig. 4b). The FT-IR spectra of the TS-1 and TS-1p display all the characteristic signals (i.e., 1220, 1100, 800, 550 and 450 cm^{-1}) of MFI zeolites as well as the peak at 965 cm^{-1} attributed to substituted titanium in the zeolite framework. The intensity of the 965

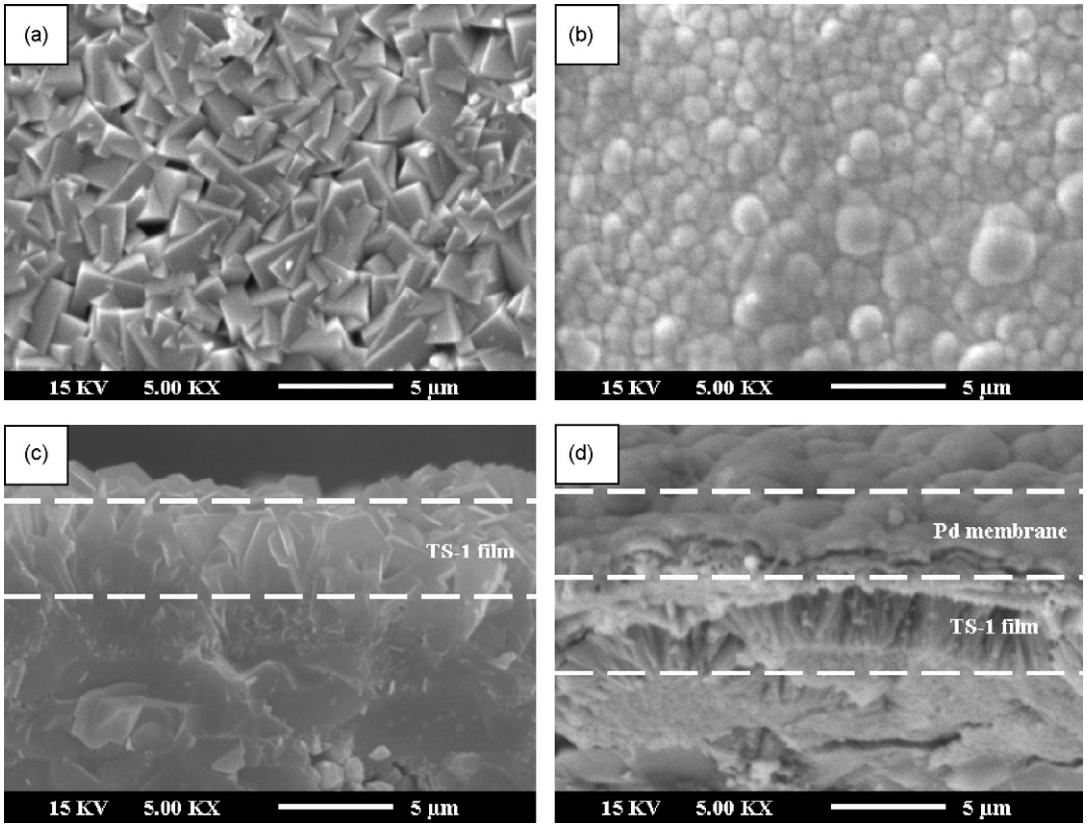

Fig. 7. SEM images of TS-1 films and Pd–TS-1 composite membrane ((a and b) surface and (c and d) cross-section).

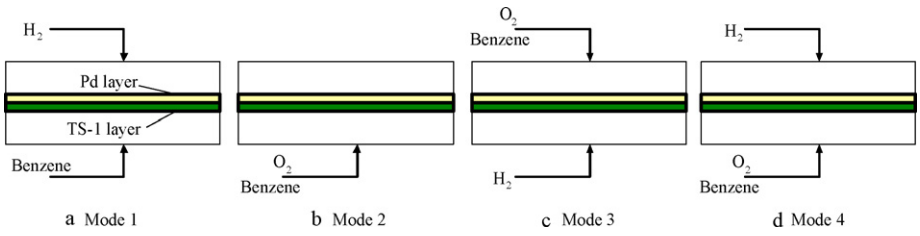

Scheme 1. Modes of reaction scheme with Pd–TS-1 composite membrane reactor.

Table 1
The catalytic performances of benzene hydroxylation on different conditions.

Reaction condition	Benzene conversion (%)	Product distribution (%)			
		Phenol	Cyclohexane	Cyclohexanone	Dihydroxybenzene
Mode 1	0.69	0	100	0	0
Mode 2	0	0	0	0	0
Mode 3	4.26	72.95	8.79	16.58	1.68
Mode 4	0.12	97.15	0	0	2.85
Mode 4-2	5.39	94.79	1.98	2.61	0.62
Pd–Sil-1	4.10	62.45	15.23	22.32	0

Mode 4-2: is similar with mode 4 except TS-1p instead of TS-1. Pd–Sil-1: is the same as the mode 3.

and 800 cm^{-1} peak increased after the TPAOH treatment, but the I_{965}/I_{800} ratio corresponding remained unchanged [44]. The UV–Vis spectra in Fig. 5b indicated that TPAOH treatment could reincorporate some of the extra-framework titanium species (Fig. 5, dotted line), but did not lead to a change in the tetra-coordinated titanium (ca. 210 nm).

It is possible to conclude that the TPAOH treatment resulted mainly in creating mesoporosity in TS-1 without significant changing the zeolites morphology (cf. Fig. 2). The overall titanium content remained unchanged after the treatment, but a redistribution of titanium species was observed. The impact of the treatment is more clearly seen in the gas permeation data in Fig. 6. The flux of N_2, O_2 and benzene/N_2 in TS-1p is about 100 times higher than TS-1 over the entire range of trans-membrane pressures studied, which is consistent with the increased porosity of the TS-1p.

3.2. Pd–TS-1 and Pd–TS-1p composite membranes

Palladium was deposited by electroless plating on the zeolites surface after seeding. Fig. 7 displays the membrane surface (Fig. 7a and b) and cross-sections (Fig. 7c and d) before and after palladium deposition. A 4 μm thick Pd was deposited on the 5 μm thick TS-1 layer as shown in Fig. 7d. The hydrogen and nitrogen permeance of TS-1 at 473 K were respectively 3.3×10^{-4} and 1.81×10^{-4} mol m^{-2} s^{-1} $Pa^{-0.5}$, and after deposition of Pd a comparable H_2 permeance of 4.4×10^{-4} mol m^{-2} s^{-1} $Pa^{-0.5}$ was obtained but the Pd–TS-1 displayed a low N_2 permeance of 6.5×10^{-6} mol m^{-2} s^{-1} $Pa^{-0.5}$. The low nitrogen permeance of Pd–TS-1 suggests low number of defects, while the identical hydrogen permeance of TS-1 and Pd–TS-1 indicates that transport resistance across the 5 μm thick TS-1 is not negligible. The hydrogen and H_2/N_2 ideal selectivity were plotted in Fig. 8 as a function of trans-membrane pressures and temperatures. The Pd–TS-1 gave sufficiently high hydrogen permeance even at 473 K with good H_2/N_2 selectivity that is adequate for the current application.

3.3. Direct hydroxylation of benzene to phenol over Pd–TS-1 membrane

The direct hydroxylation of aromatic compounds in palladium membrane reactor is considered an attractive alternative for the production of phenol from benzene [8–12]. The purpose of this

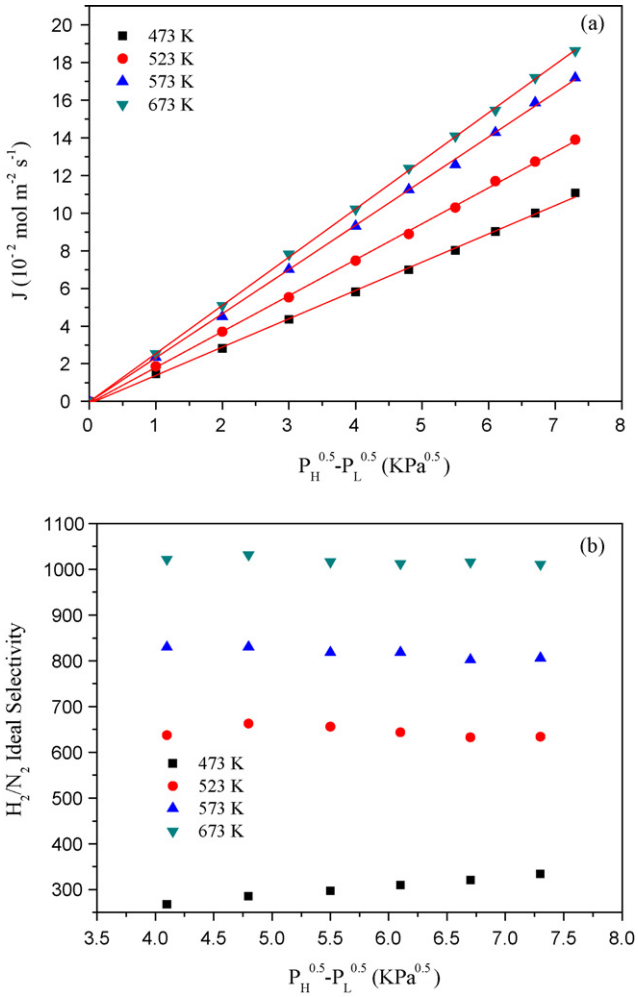

Fig. 8. Hydrogen flux (a) and nitrogen (b) flux H_2/N_2 ideal selectivity (b) through Pd membrane as a function of pressure at different temperatures.

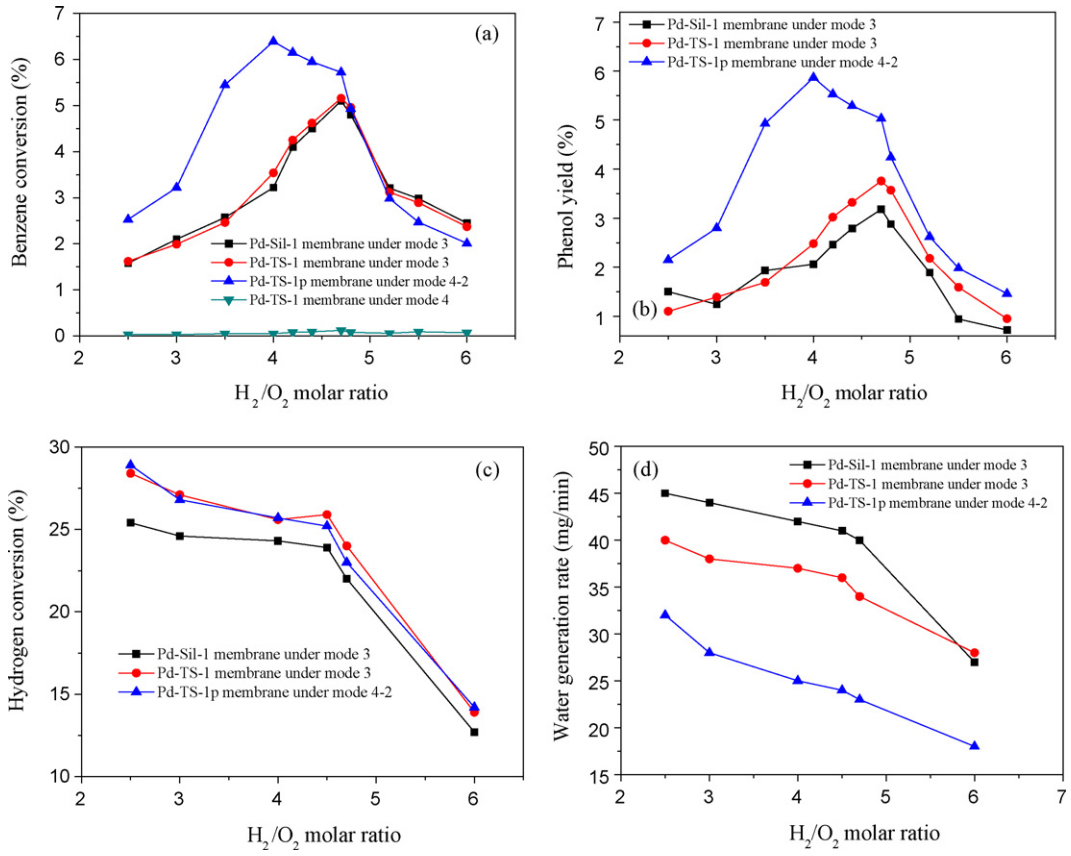

Fig. 9. The reaction properties of benzene conversion (a), phenol yield (b), hydrogen efficiency (c) and water generation (d) as a function of H_2/O_2 molar ratio on the different membrane reactors.

work is to improve hydrogen utilization and product yield by adding a zeolites catalyst layer to the Pd membrane. The effects of reactor configuration (see Scheme 1) were examined.

3.3.1. *Reactor configurations*

Reactor mode 1 fed the benzene/nitrogen mixture to the TS-1 zeolite on the support side, while hydrogen was fed on the Pd membrane-side as shown in Scheme 1a. This reactor configuration produced mainly cyclohexane from the hydrogenation of benzene over the Pd–TS-1 membrane (Table 1). Reactor mode 2 co-fed benzene/N_2 and oxygen to the TS-1 zeolite on the support side as shown in Scheme 1b. No reaction was observed under this operating condition and TS-1 is inactive for the direct oxidation of benzene by molecular oxygen. It is clear from the results that TS-1 cannot catalyze direct hydroxylation of benzene with either hydrogen or oxygen gas alone. The reactor mode 3 fed hydrogen to the TS-1 zeolite on the support side and benzene/O_2/N_2 mixture to the Pd membrane-side as shown in Scheme 1c. Phenol was the main product of the reaction (4.26% yield, 72.95% selectivity) with dihydroxybenzene, cyclohexane and cyclohexanone as by-products (Table 1). The reactor mode 4 fed the benzene/O_2/N_2 mixture to the TS-1 zeolite on the support side and hydrogen to the Pd membrane-side (Scheme 1d). This configuration was expected to led to higher conversion and product yield, but the results show that for the Pd–TS-1 composite membrane that the conversion was very low (i.e., 0.1%) although a product selectivity of 97% was obtained.

3.3.2. *H_2/O_2 molar feed ratio*

It was speculated that this is due to slow diffusion of the reactants and product through the TS-1 zeolite. The reactor mode 4 was repeated for a Pd–TS-1p (Mode 4-2 in Table 1) composite membrane where the TS-1 zeolite was pretreated with TPAOH to introduce mesopores and decrease the mass transport resistance in the zeolites layer (cf. Fig. 6). A benzene conversion of 5.4% and phenol selectivity of 95% were obtained. Fig. 9 plots the benzene conversion (Fig. 9a), phenol yield (Fig. 9b), hydrogen conversion (Fig. 9c) and water generation (Fig. 9d) as a function of H_2/O_2 molar feed ratio for Pd–TS-1, Pd–TS-1p and Pd–Sil-1 membranes operated under reactor modes 3 and 4. The benzene conversions of Pd–TS-1 and Pd–Sil-1 operated in reactor mode 3 are comparable and display a maximum at H_2/O_2 molar feed ratio of 4.7. This suggests that the zeolites layer did not participate in the catalytic conversion of benzene which is also indicated by the plot of phenol yield in Fig. 9b. This is reasonable as the hydroxylation reaction happens on the Pd surface in this reactor configuration (see Scheme 1c).

The hydroxylation reaction occurs in the zeolite layer under reaction mode 4 as shown in Scheme 1d. In this case, the nature of the zeolite catalyst is important. Slow diffusion in the TS-1 zeolite results in low benzene conversion (Fig. 9a) and phenol yield (Fig. 9b) regardless of the H_2/O_2 molar feed ratio. Replacing the TS-1 with TS-1p in Pd–TS-1p composite membrane results in immediate increase in benzene conversion and phenol yield. The optimum H_2/O_2 molar feed ratio is 4 lower than the Pd–TS-1 and Pd–Sil-1 ran under reactor mode 3. This gives strong evidence that TS-1p layer catalyzed the reaction, which is further supported by hydrogen conversion and water generation results in Fig. 9c and d. The hydrogen conversion is significantly lower for Pd–TS-1p membrane (ca. 25% at $H_2/O_2 = 4$) as compared to Pd–TS-1 and Pd–Sil-1 membranes, which have 27% hydrogen conversion at H_2/O_2 of 4.7. Water production is dramatically lower in Pd–TS-1p membrane and is less than half of Pd–Sil-1 membrane.

The reaction results indicate that the direct hydroxylation of benzene requires both hydrogen and oxygen co-reactant. The Pd

membrane can catalyze the conversion of benzene to phenol as reported by Niwa et al. [8] and the reaction is sensitive to the H_2/O_2 molar feed ratio. The optimum H_2/O_2 molar feed ratio is governed by membrane permeation rate, reactant composition and reaction conditions, and changes accordingly. Besides phenol, water, cyclohexanone, cyclohexane and carbon dioxide are major by-products when reactions occurred on the Pd membrane as in the case of Pd–TS-1 and Pd–Sil-1 membrane operated in reactor mode 3. Benzene conversion to phenol is also catalyzed by TS-1 and TS-1p catalysts according to the reaction results from reactor mode 4. These catalysts are active for the hydroxylation of aromatics by H_2O_2 as reported in our recent works [29,30]. Superb selectivity to phenol was obtained from both Pd–TS-1 and Pd–TS-1p. The TS-1 and TS-1p catalysts also suppressed water production and improved hydrogen utilization efficiency. The lower transport resistance in TS-1p is responsible for the higher reaction conversion and product yield observed in Pd–TS-1p membrane. It is postulated that the ability of zeolite catalyst to stabilize the reactive species generated from reactions between permeated hydrogen ions and molecular oxygen is responsible for the enhanced reaction.

4. Conclusion

This work demonstrates that it is possible to improve the direct hydroxylation of benzene in Pd membrane reactor by incorporating TS-1 catalyst. Reactor configuration, reactant composition and reaction conditions are shown to be important to the reaction. Large intra-crystalline voids and mesopores in TS-1p were obtained by simply treating the TS-1 with TPAOH. The TS-1p had better catalytic activity for benzene hydroxylation by H_2O_2 compared to untreated TS-1 due to improved diffusion and elimination of extra-framework titanium. The Pd–TS-1 and Pd–TS-1p membrane were prepared by electroless plating Pd and display high selectivity for phenol (>95%) compared to Pd–Sil-1 (ca. 65%). Faster diffusion in mesoporous TS-1p results in higher benzene conversion in Pd–TS-1p (ca. 5.4%) as compared to Pd–TS-1 (ca. 0.1%). The TS-1 and TS-1p catalysts suppressed water production and increased hydrogen utilization efficiency. Although the benzene conversion and phenol yield remain low compared to the literature report, we believe that this is mainly due to poorer mass transfer in the large diameter membrane used in this study compared to capillary membranes employed in prior works [8–13], and indeed the use of MEMS-based Pd microreactor gave benzene conversion of up to 54% and phenol yield of 20% [45]. Miniaturization can significantly improve mass transfer and results in better reaction performance [46–53].

Acknowledgements

The authors gratefully acknowledge financial support provided by National Natural Science Foundation of China (Grant No. 20673017), PetroChina Innovation Foundation (Grant No. 2008D-5006-05-06), China National 863 Program (Grant No. 2007AA05Z137) and Universities Science & Research Project of Liaoning Province Education Department (Grant No. 2009S019).

References

[1] M. Stockmann, F. Konietzni, J.U. Notheis, J. Voss, W. Keune, W.F. Maier, Appl. Catal. A: Gen. 208 (2001) 343–358.
[2] D. Bianchi, R. Bortolo, R. Tassinari, M. Ricci, R. Vignola, Angew. Chem. Int. Ed. 39 (2000) 4321–4323.
[3] B. Louis, L. Kiwi-Minsker, P. Reuse, A. Renken, Ind. Eng. Chem. Res. 40 (2001) 1454–1459.
[4] L.V. Pirutko, V.S. Chernyavsky, A.K. Uriarte, G.I. Panov, Appl. Catal. A: Gen. 227 (2002) 143–157.
[5] T. Miyake, M. Hamada, Y. Sasaki, M. Oguri, Appl. Catal. A: Gen. 131 (1995) 33–42.
[6] N.I. Kuznetsova, L.I. Kuznetsova, V.A. Likholobov, G.P. Pez, Catal. Today 99 (2005) 193–198.
[7] W. Laufer, W.F. Hoelderich, Chem. Commun. (2002) 1684–1685.
[8] S. Niwa, M. Eswaramoorty, J. Nair, A. Raj, N. Itoh, H. Shoji, T. Namba, F. Mizukami, Science 295 (2002) 105–107.
[9] G.D. Vulpescu, M. Ruitenbeek, L.L. van Lieshout, L.A. Correia, D. Meyer, P.P.A.C. Pex, Catal. Commun. 5 (2004) 347–351.
[10] N. Itoh, S. Niwa, F. Mizukami, T. Inoue, A. Igarashi, T. Namba, Catal. Commun. 4 (2003) 243–246.
[11] K. Sato, T. Hanaoka, S. Niwa, C. Stefan, T. Namba, F. Mizukami, Catal. Today 104 (2005) 260–266.
[12] K. Sato, T. Hanaoka, S. Hamakawa, M. Nishioka, K. Kobayashi, T. Inoue, T. Namba, F. Mizukami, Catal. Today 118 (2006) 57–62.
[13] E.E. McLeary, J.C. Jansen, F. Kapteijn, Micropor. Mesopor. Mater. 90 (2006) 198–220.
[14] S.M. Lai, R. Martin-Aranda, K.L. Yeung, Chem. Commun. (2003) 218–219.
[15] S.M. Lai, C.P. Ng, R. Martin-Aranda, K.L. Yeung, Micropor. Mesopor. Mater. 66 (2003) 239–252.
[16] X.F. Zhang, E.S.M. Lai, R. Martin-Aranda, K.L. Yeung, Appl. Catal. A: Gen. 261 (2004) 109–118.
[17] W.N. Lau, K.L. Yeung, R. Martin-Aranda, Micropor. Mesopor. Mater. 115 (2008) 156–163.
[18] G. Bellussi, A. Carati, M.G. Clerici, G. Maddinelli, R. Millini, J. Catal. 133 (1992) 220–230.
[19] M.G. Clerici, P. Ingallina, J. Catal. 140 (1993) 71–83.
[20] P. Wu, T. Komatsu, T. Yashima, J. Phys. Chem. B 102 (1998) 9297–9303.
[21] P. Chen, X.B. Chen, X.S. Chen, H. Kita, J. Membr. Sci. 330 (2009) 369–378.
[22] X.D. Wang, B.Q. Zhang, X.F. Liu, J.Y.S. Lin, Adv. Mater. 18 (2006) 3261–3265.
[23] X.D. Wang, P.P. Zhang, X.F. Liu, B.Q. Zhang, Appl. Surf. Sci. 15 (2007) 544–547.
[24] P. Chen, X.S. Chen, K. Tanaka, H. Kita, Chem. Lett. 36 (2007) 1078–1079.
[25] Q. Zhao, P. Li, D.Q. Li, X.G. Zhou, W.K. Yuan, X.J. Hu, Micropor. Mesopor. Mater. 108 (2008) 311–317.
[26] Y.S.S. Wan, J.L.H. Chau, A. Gavriilidis, K.L. Yeung, Chem. Commun. (2002) 978–979.
[27] Y.S.S. Wan, J.L.H. Chau, A. Gavriilidis, K.L. Yeung, J. Catal. 223 (2004) 241–249.
[28] Y.S.S. Wan, K.L. Yeung, A. Gavriilidis, Appl. Catal. A: Gen. 281 (2005) 285–293.
[29] X.B. Wang, X.F. Zhang, H.O. Liu, K.L. Yeung, J.Q. Wang, Chem. Eng. J. 156 (2010) 562–570.
[30] F.R. Qiu, X.B. Wang, X.F. Zhang, H.O. Liu, S.Q. Liu, K.L. Yeung, Chem. Eng. J. 147 (2009) 316–322.
[31] J.L.H. Chau, C. Tellez, K.L. Yeung, K.C. Ho, J. Membr. Sci. 164 (2000) 257–275.
[32] S.M. Lai, L.T.Y. Au, K.L. Yeung, Micropor. Mesopor. Mater. 54 (2002) 63–77.
[33] W.C. Wong, L.T.Y. Au, C. Tellez, K.L. Yeung, J. Membr. Sci. 191 (2001) 143–163.
[34] L.T.Y. Au, W.Y. Mui, P.S. Lau, C. Tellez, K.L. Yeung, Micropor. Mesopor. Mater. 47 (2001) 203–216.
[35] L.T.Y. Au, K.L. Yeung, J. Membr. Sci. 194 (2001) 33–55.
[36] W.C. Wong, L.T.Y. Au, P.P.S. Lau, C. Tellez, K.L. Yeung, J. Membr. Sci. 193 (2001) 141–161.
[37] K.L. Yeung, R. Aravind, J. Szegner, A. Varma, Stud. Surf. Sci. Catal. 101 (1996) 1349–1358.
[38] K.L. Yeung, S.C. Christiansen, A. Varma, J. Membr. Sci. 159 (1999) 107–122.
[39] Y.S. Cheng, K.L. Yeung, J. Membr. Sci. 182 (2001) 195–203.
[40] Y.S. Cheng, K.L. Yeung, J. Membr. Sci. 158 (1999) 127–141.
[41] Y.S. Cheng, M.A. Peña, J.L. Fierro, D.C.W. Hui, K.L. Yeung, J. Membr. Sci. 204 (2002) 329–340.
[42] M. Ogura, S.Y. Shinomiya, J. Tateno, Y. Nara, M. Nomura, E. Kikuchi, M. Matsukata, Appl. Catal. A: Gen. 219 (2001) 33–43.
[43] Y.R. Wang, M. Lin, A. Teul, Micropor. Mesopor. Mater. 102 (2007) 80–85.
[44] D.P. Serrano, M.A. Uguina, G. Ovejero, R. Van Grieken, M. Camacho, Micropor. Mater. 4 (1995) 273–282.
[45] S.-Y. Ye, S. Hamakawa, S. Tanaka, K. Sato, M. Esashi, F. Mizukami, Chem. Eng. J. 155 (2009) 829–837.
[46] J.L.H. Chau, Y.S.S. Wan, A. Gavriilidis, K.L. Yeung, Chem. Eng. J. 88 (2002) 187–200.
[47] J.L.H. Chau, K.L. Yeung, Chem. Commun. (2002) 960–961.
[48] J.L.H. Chau, A.Y.L. Leung, K.L. Yeung, Lab Chip 3 (2003) 53–55.
[49] A.Y.L. Leung, K.L. Yeung, Chem. Eng. Sci. 59 (2004) 4809–4817.
[50] S.M. Kwan, K.L. Yeung, Chem. Commun. (2008) 3631–3633.
[51] Y.S.S. Wan, A. Gavriilidis, K.L. Yeung, Chem. Eng. Res. Des. 81 (2003) 753–759.
[52] K.L. Yeung, X.F. Zhang, W.N. Lau, R. Martin-Aranda, Catal. Today 110 (2005) 26–37.
[53] K.L. Yeung, S.M. Kwan, W.N. Lau, Top. Catal. 52 (2009) 101–110.